

Issues in Understanding Collisionless Shocks in the Heliosphere

J. R. Jokipii
University of Arizona

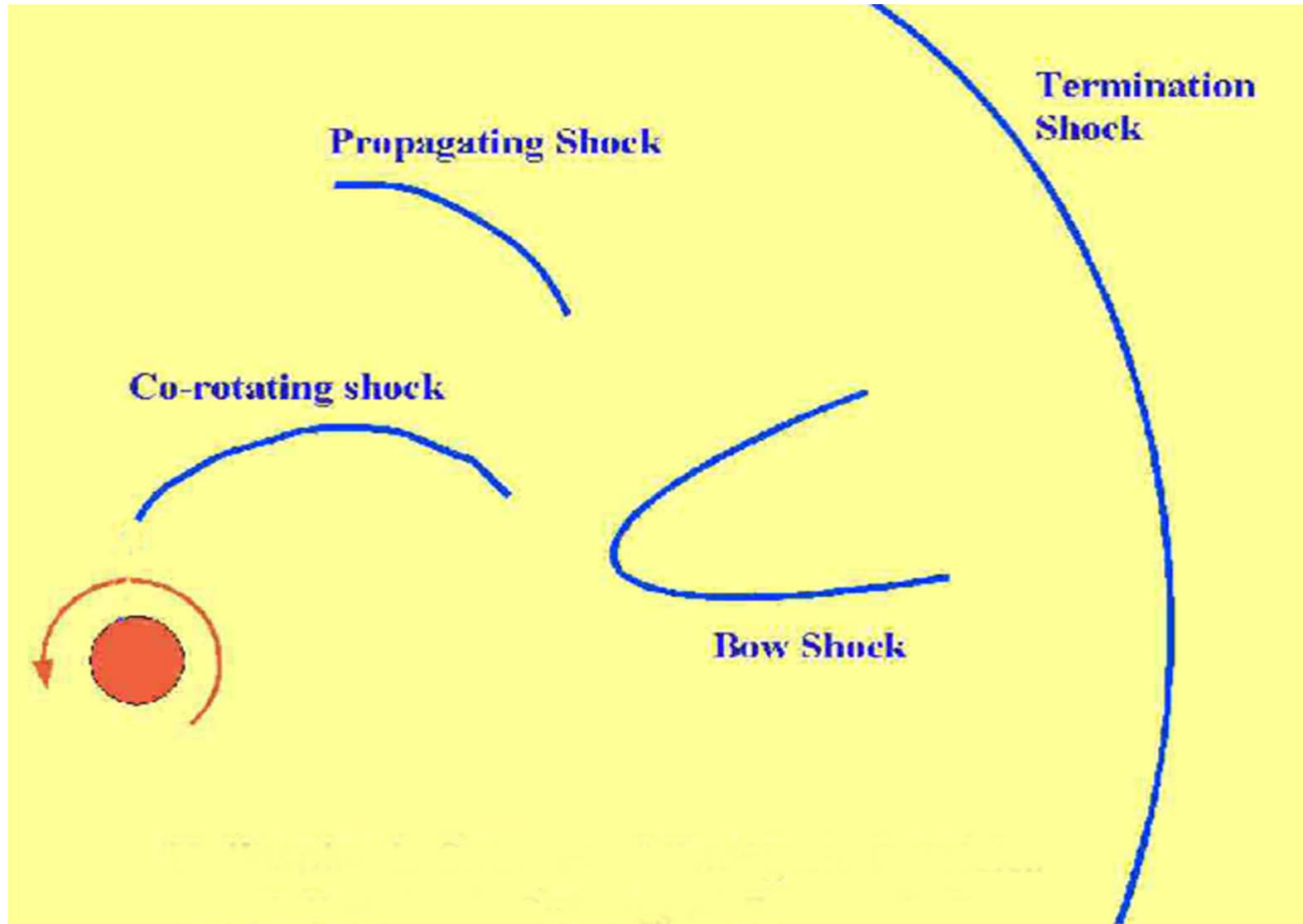
Acknowledgements to my Arizona
Colleagues, Joe Giacalone and Jozsef Kóta .

*Presented at the WOPA , Princeton, N.J.
January 18, 2010*

Outline of Talk

- General Background Regarding Heliospheric Shocks
 - Taxonomy of heliospheric shocks.
 - Energetic particles and shocks.
- Current major issues:
 - Particle acceleration at quasi-perpendicular shocks – the injection problem.
 - The role of large-scale, upstream turbulence.

Shocks in the heliosphere



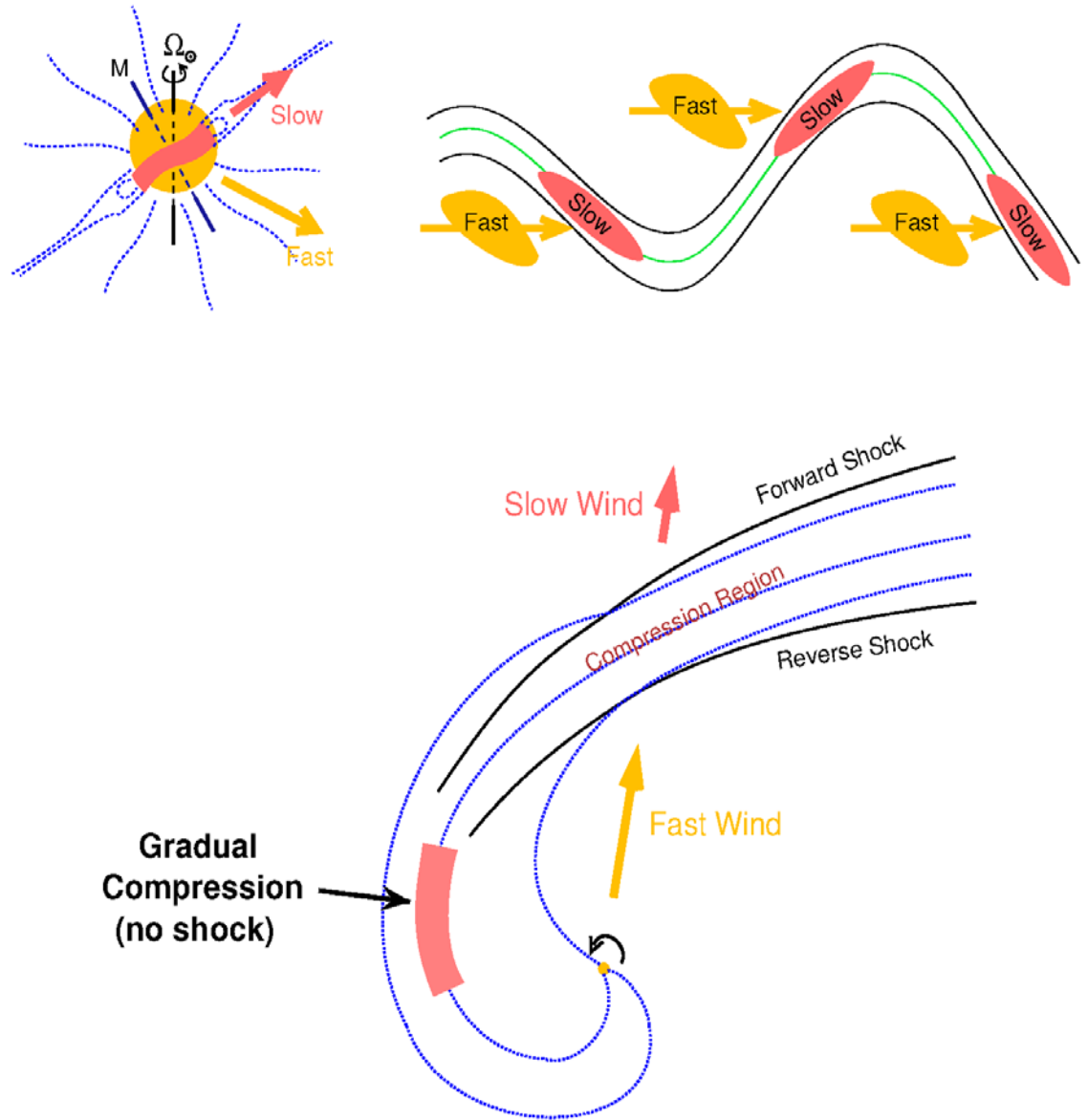
Each shock is a source of energetic particles. Some with energies up to several GeV.

Energetic Particles and Shocks

- Collisionless shocks always produce energetic particles. These are generally isotropic in pitch angle.
- The particle spectrum produced is generally a power law up to a time-dependent or geometry-related cutoff.
- The power-law index is in a narrow range (“universal”) and insensitive to parameters, as is observed.
- Energetic particles are often well-described by the Parker equation, even at shocks, since they are nearly always observed to be nearly isotropic.

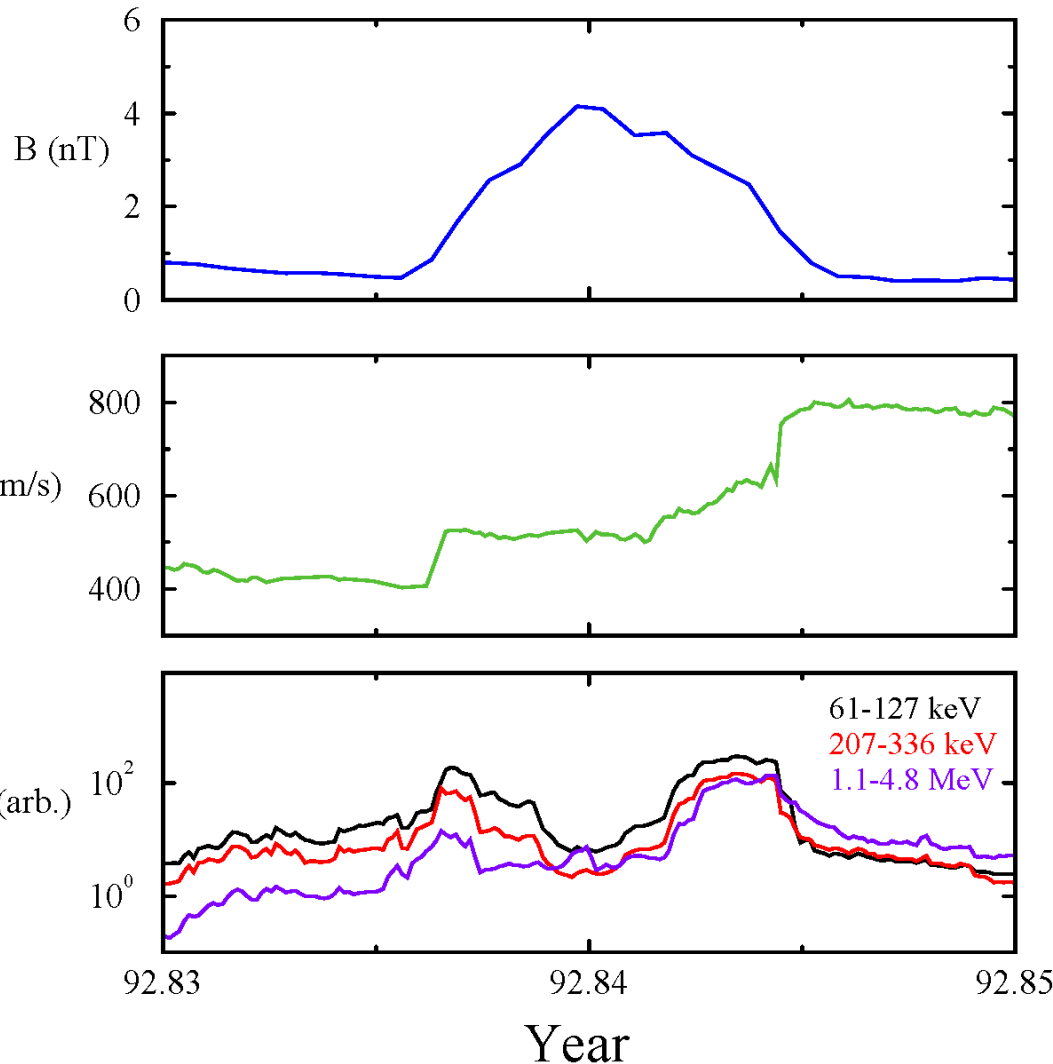
Co-rotating Interaction Regions

Example: Co-rotating interaction regions in the solar wind form shocks.



Co-rotating particle events.

Ulysses data



Compression of the magnetic field within CIR.

Slow, intermediate, and fast wind and both a Forward (F) and Reverse (R) shock.

Energetic Particles peaking at The F/R shocks, with a *larger* intensity at the reverse shock.

The Parker Equation – first order in w/U

$$\begin{aligned} \frac{\partial f}{\partial t} = & \frac{\partial}{\partial x_i} \left[\kappa_{ij}^{(S)} \frac{\partial f}{\partial x_j} \right] & \Rightarrow \text{Diffusion} \\ & - \mathbf{U} \cdot \nabla f & \Rightarrow \text{Convection w. plasma} \\ & - \mathbf{V}_d \cdot \nabla f & \Rightarrow \text{Grad \& Curvature Drift} \\ & + \frac{1}{3} \nabla \cdot \mathbf{U} \left[\frac{\partial f}{\partial \ln p} \right] & \Rightarrow \text{Energy change} \\ & + Q & \Rightarrow \text{Source} \end{aligned}$$

Where the drift velocity due to the large scale curvature and gradient of the average magnetic field is:

$$\mathbf{V}_d = \frac{pcw}{3q} \nabla \times \left[\frac{\mathbf{B}}{B^2} \right]$$

This is well-tested and established. Not useful at low particle speeds $w < \sim U$. Can be applied to shocks.

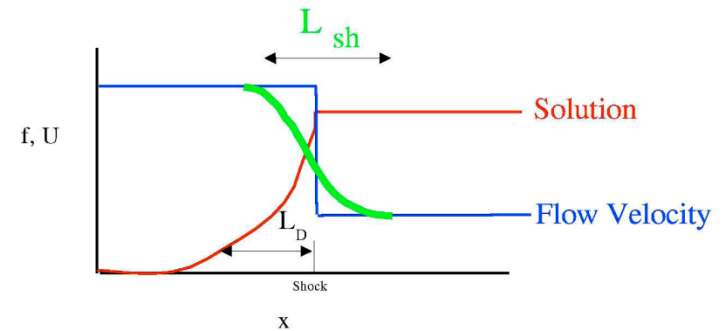
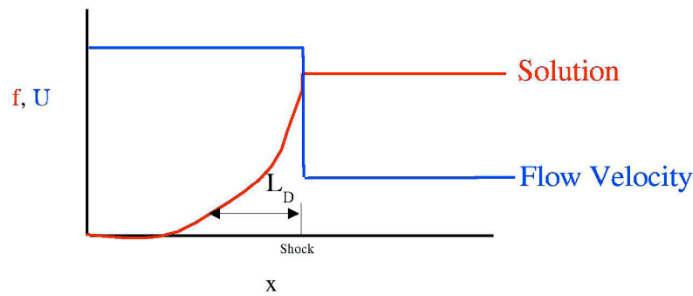
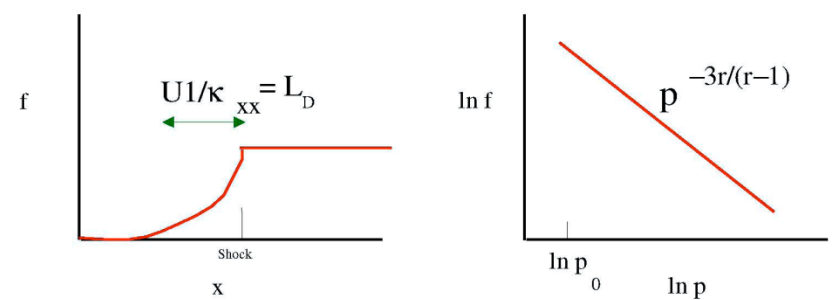
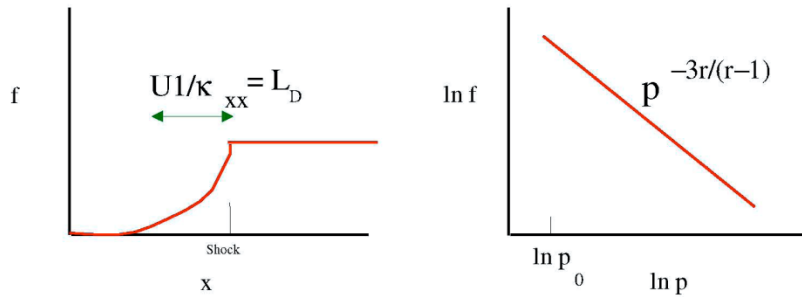


Illustration of the time-asymptotic solution to Parker's equation for a one-dimensional shock.

The spectrum is a power law in momentum with index depending *only* on the shock ratio r .

This predicted behavior is observed at shocks. This led to the well-established paradigm of diffusive shock acceleration. It explained a lot, including the universal energy spectrum.

Kennel, et al,

Unfortunately, this classic observation is not easy to repeat.

Apparently even Kennel et al were forced to look at many shocks before finding the one illustrated.

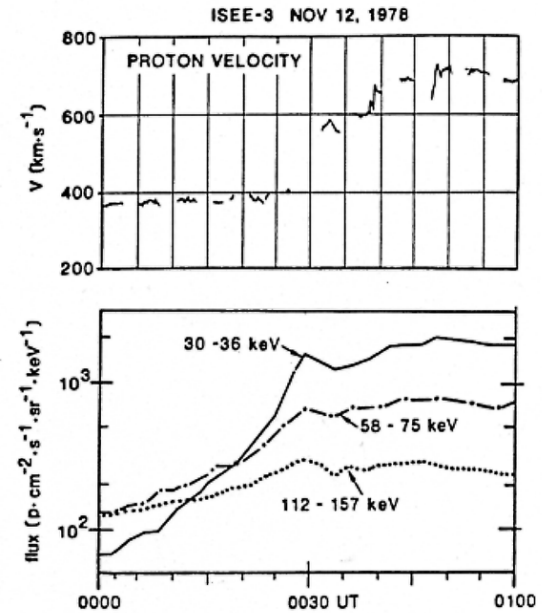
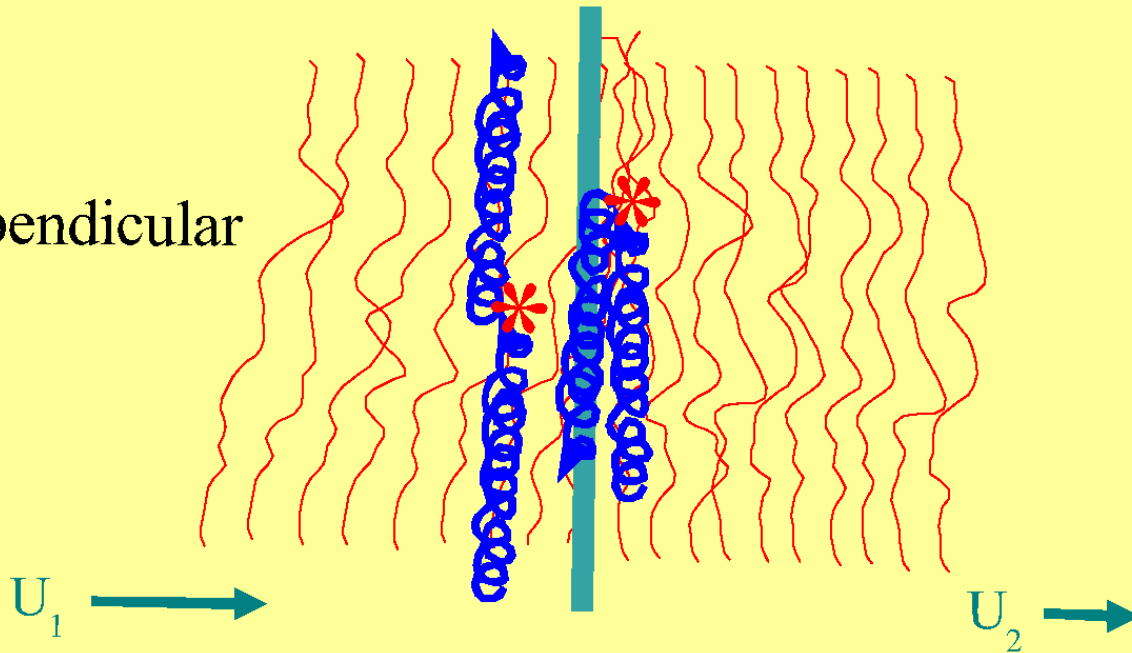


Fig. 1. Solar wind flow speed and energetic protons. The top panel shows the solar wind speed measured by the ISEE-3 solar wind plasma instrument [Bame et al., 1978] and the bottom panel shows the differential fluxes of 30–36 keV, 58–75 keV, and 112–157 keV protons measured by the ISEE-3 nuclear and ionic charge distribution Experiment [Hovestadt et al., 1978]. The period 0000–0100 UT on November 12, 1978, includes the passage of the interplanetary shock over ISEE-3 at 0028:16 UT. The solar wind proton bulk velocity increased slightly, from 380 km s⁻¹ to 400 s⁻¹, upstream of the shock and increased to 571 km s⁻¹ at the first downstream measurement. The energetic proton fluxes increased roughly exponentially ahead of the shock, with a scale length that increased with increasing energy. The fluxes maximized at the shock, and remained approximately constant downstream of the shock.

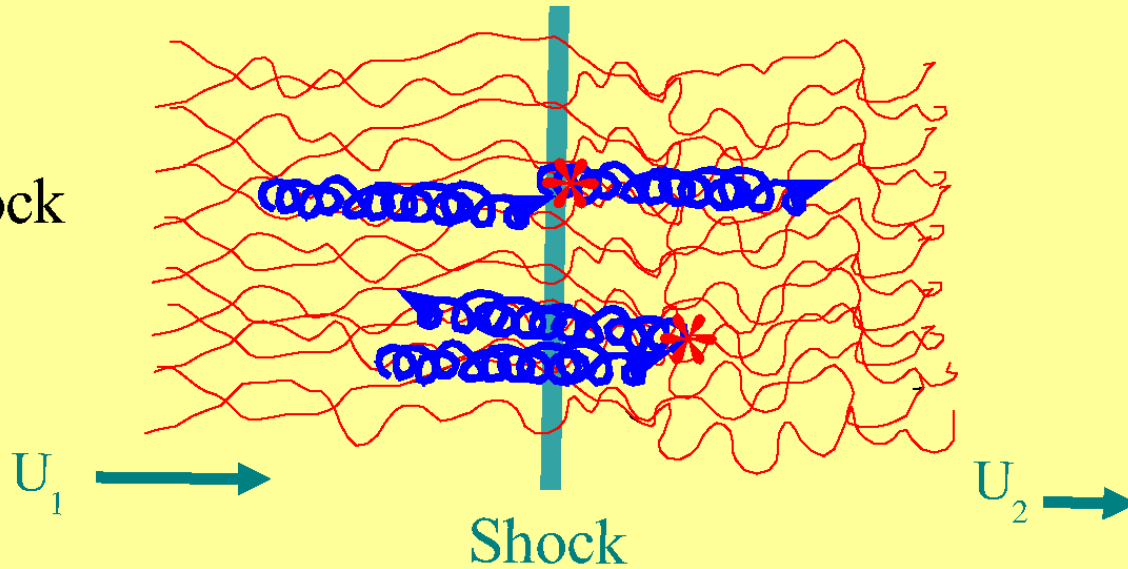
Perpendicular vs Parallel Shocks

Shock

Nearly-Perpendicular Shock



Parallel Shock

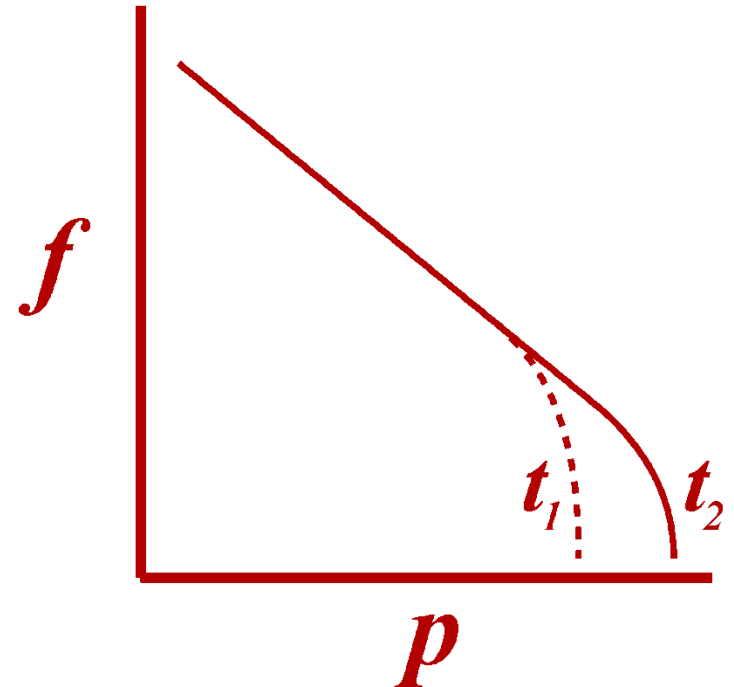


Shock

The maximum energy

- The energy is limited by both the size and age of the system
- Acceleration takes time. The ideal power-law energy spectrum is not created instantly.
 - Parallel shocks \rightarrow slow
 - Perpendicular shocks \rightarrow fast
- The maximum energy over a given time interval strongly depends on the shock-normal angle

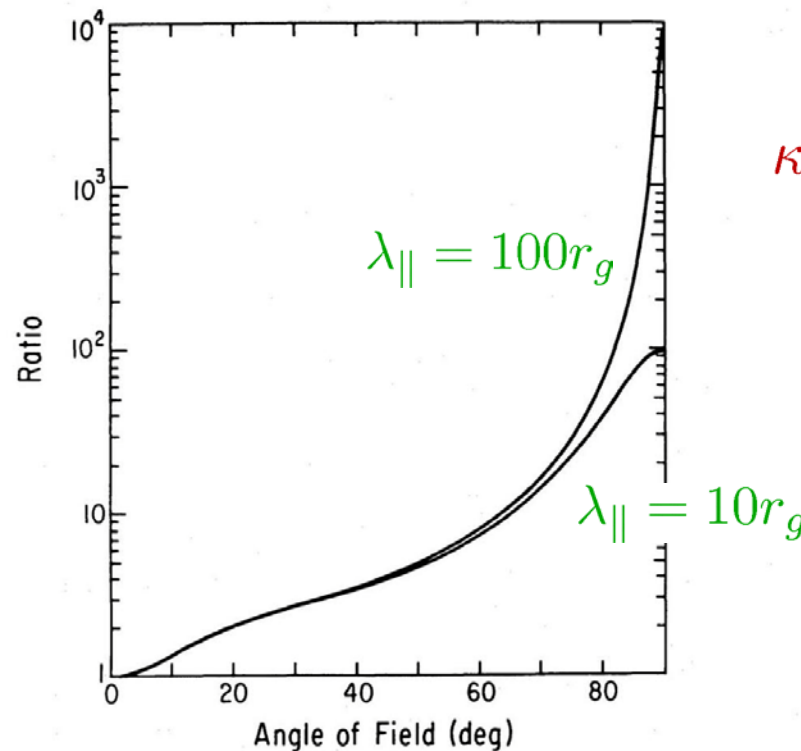
for any given situation, a perpendicular shock will yield a larger maximum energy than a parallel shock.



Acceleration Rate as a Function of Shock–Normal Angle: (assumes the billiard–ball approximation)

The acceleration rate depends inversely on the diffusion coefficient

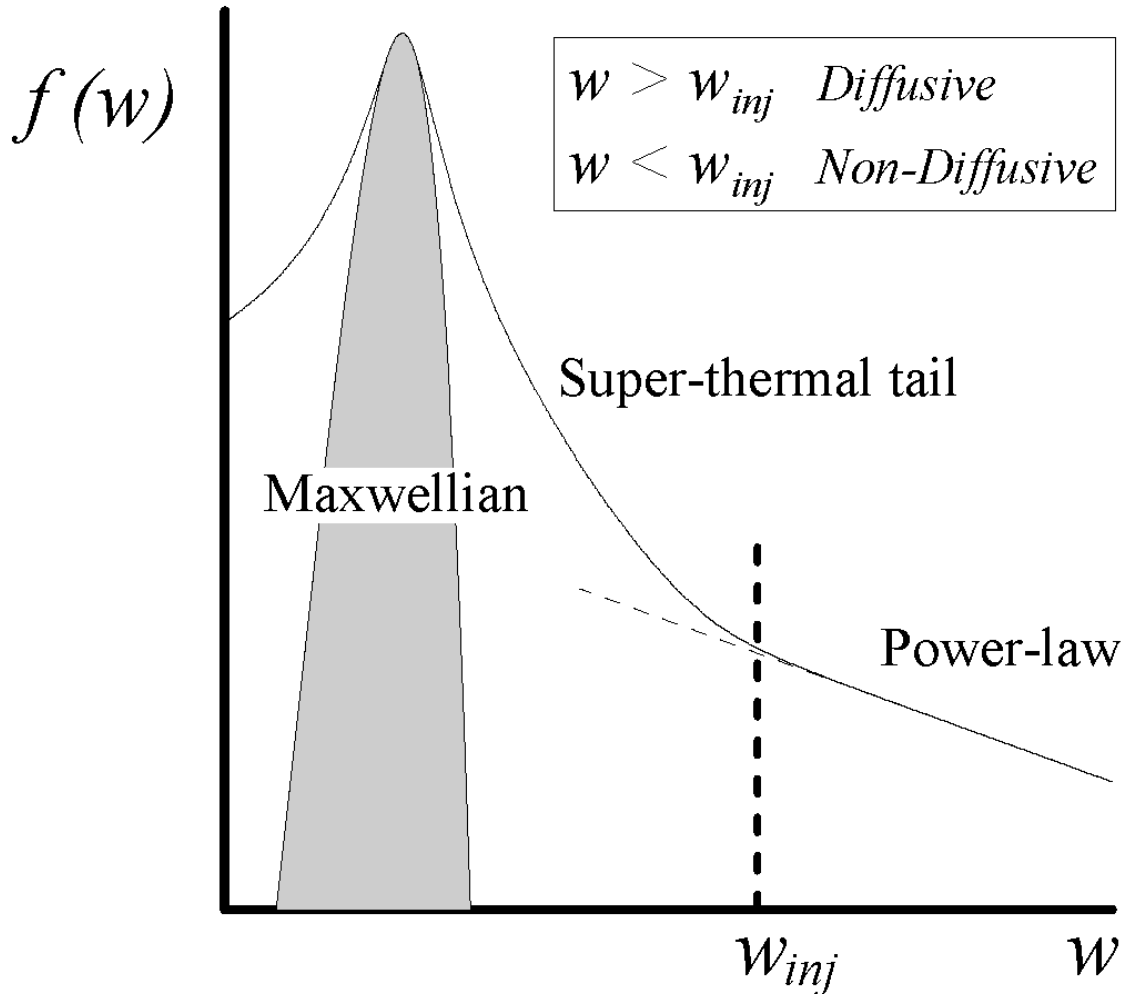
$$\frac{1}{\tau_{acc}} \propto \frac{U_{sh}^2}{\kappa_{xx}}$$



$$\kappa_{\perp} = \left(\frac{r_g}{\lambda_{\parallel}} \right)^2 \kappa_{\parallel}$$

FIG. 1.—Plot of the ratio of energy gain rate with a transverse magnetic field to that neglecting the magnetic field given in eq. (8), as a function of angle between the upstream magnetic field and shock normal, θ_1 . The upper curve is for a scattering mean free path λ_{\parallel} equal to 100 times the gyroradius r_g , and the lower is for $\lambda_{\parallel} = 10 r_g$.

Acceleration at low energies: The injection problem



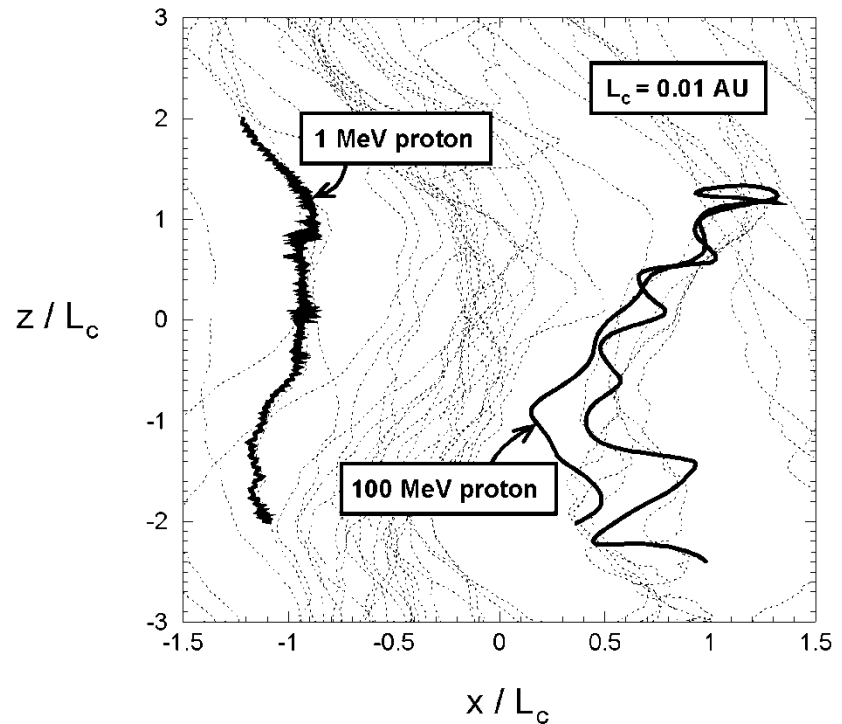
The limit of diffusive shock acceleration

- An often-invoked injection criterion is

$$v_{inj} > U_{sh} \sec \theta_{Bn}$$

- This assumes, for no good reason, that there is NO motion normal the average magnetic field
- This expression has led to a widely held misconception that perpendicular shocks are inefficient accelerators of particles

- In general, particles move normal to magnetic fields.
 - Field-line random walk leads to a larger diffusion coefficient that expected from hard-sphere scattering
 - Numerical simulations show that $\kappa_{\perp}/\kappa_{\parallel}$ is large and nearly independent of energy
- The injection criterion must be re-derived to include perpendicular diffusion



With this general picture, a general consensus arose that diffusive Shock acceleration was a well-established phenomenon that, *with few exceptions*, agreed with energetic-particle observations.

It became a possible 'universal' accelerator, applied from the heliosphere to intergalactic space.

However, in reality, often the *in situ* observed energy spectrum, at a given observer, does not agree with theory, and the accelerated particles were often not even observed to peak at the shock crossing

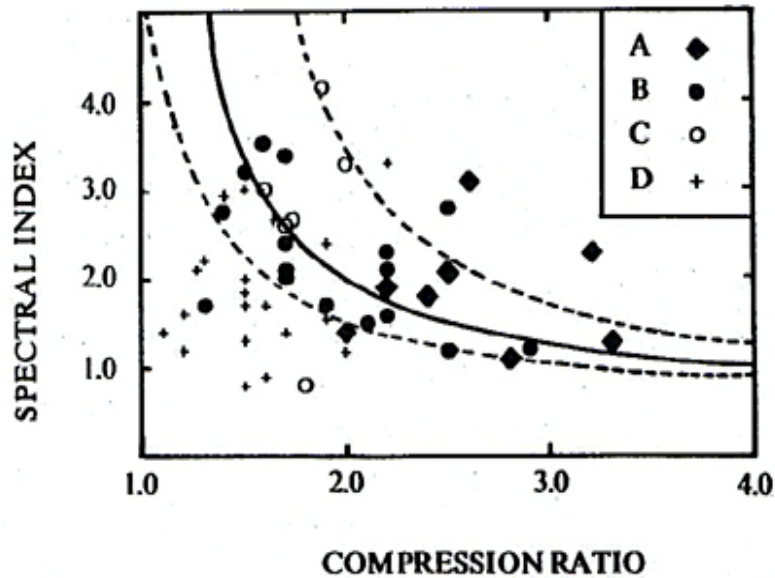


Fig. 12. Spectral index γ plotted as a function of the hydrodynamic shock strength H . The index was derived for the spectrum constructed from the average flux during 10 min immediately after the shock passage. The solid curve indicates the theoretical relation $\gamma = (H + 2)(2H - 2)^{-1}$. Points within the dashed lines are considered to follow the relation, because of the uncertainty of 25% in H . The events from the different classes are distinguished by different symbols.

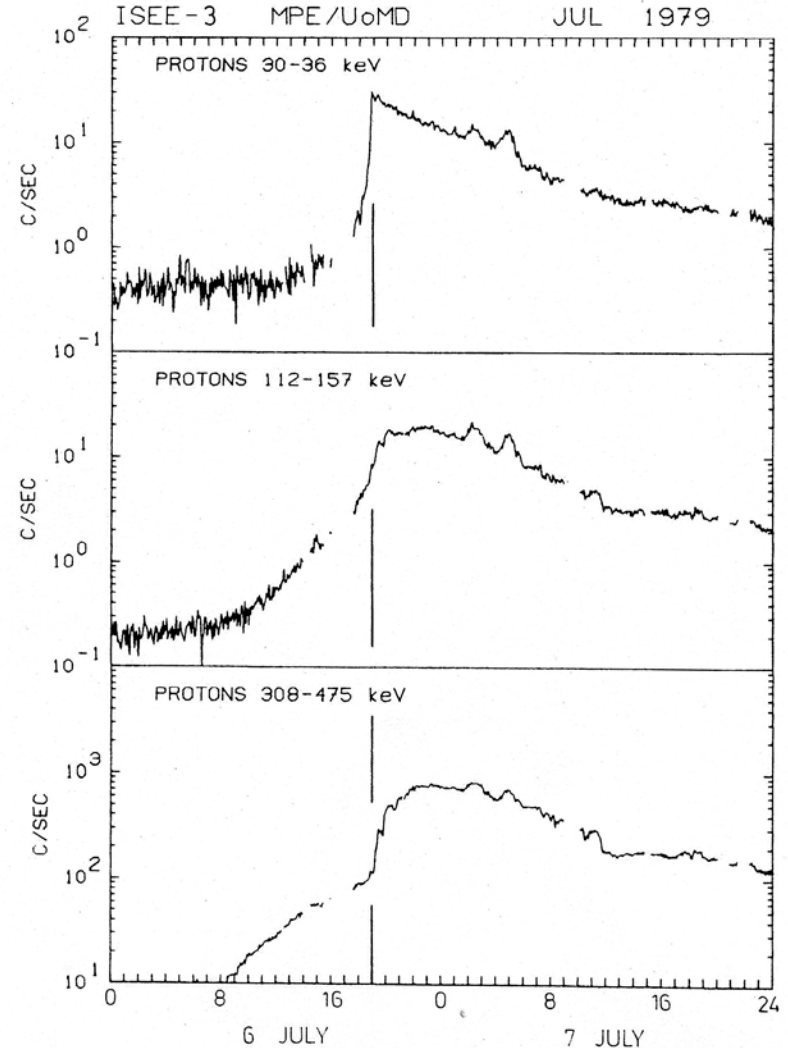


Fig. 10. Intensity-time profiles of low energy protons in three different energy intervals during the July 6-7, 1979, interplanetary shock event. Solid line shows the time of the shock passage.

Hence the nice picture of shock acceleration was too simple.

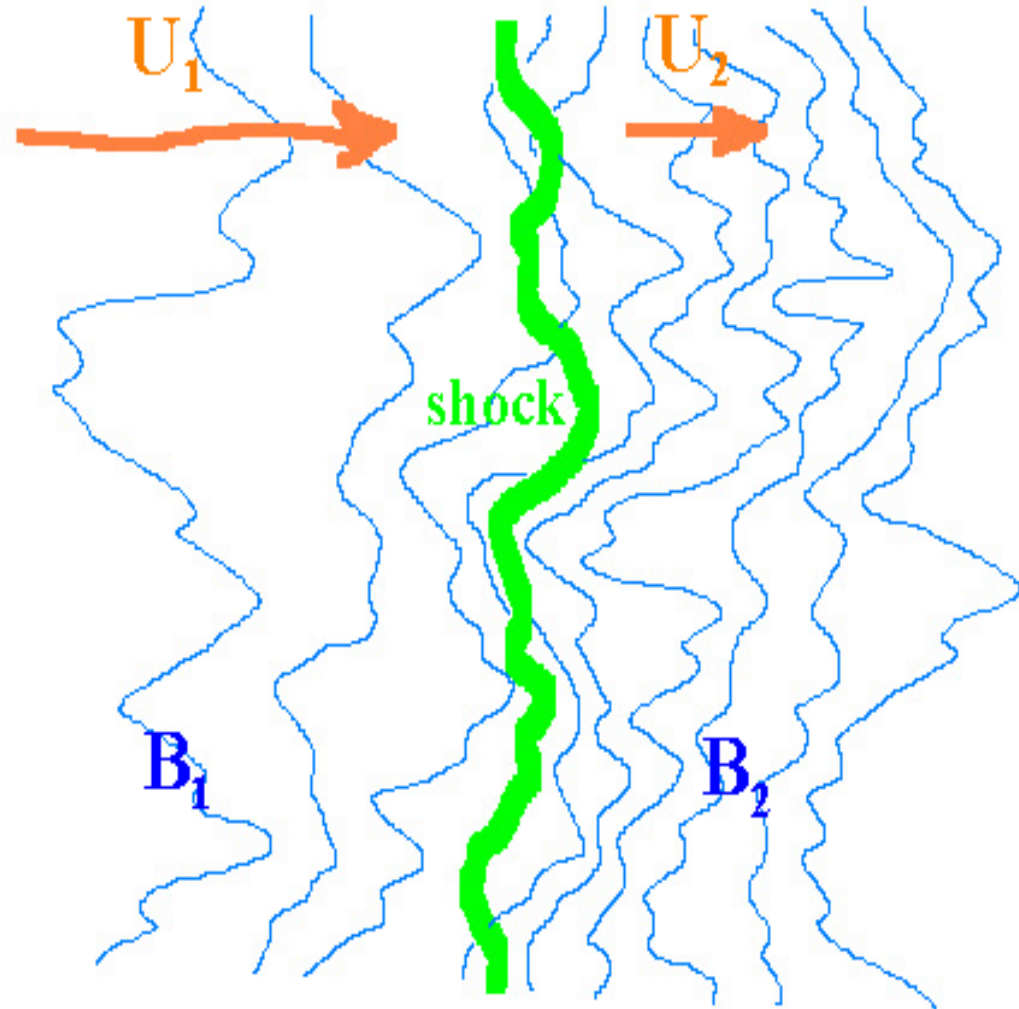
- It did not agree with many, if not most, observations of energetic particles at propagating shocks.
- An attractive interpretation of these various observations is that they are related to the pre-existing upstream turbulence and related fluctuations.
 - The propagation of the shock waves through the ubiquitous large-scale turbulence in the plasmas causes significant, changes to the shock which are essentially unpredictable.
 - The properties of individual shock waves vary in important ways both along the shock face and as a function of time along the shock.
 - Different spacecraft crossing the same shock at different points will generally see quite different phenomena.

These phenomena are best studied statistically, just like turbulence itself, using data from multiple shock crossings, by multiple spacecraft.

A tidal bore is a good analogy.

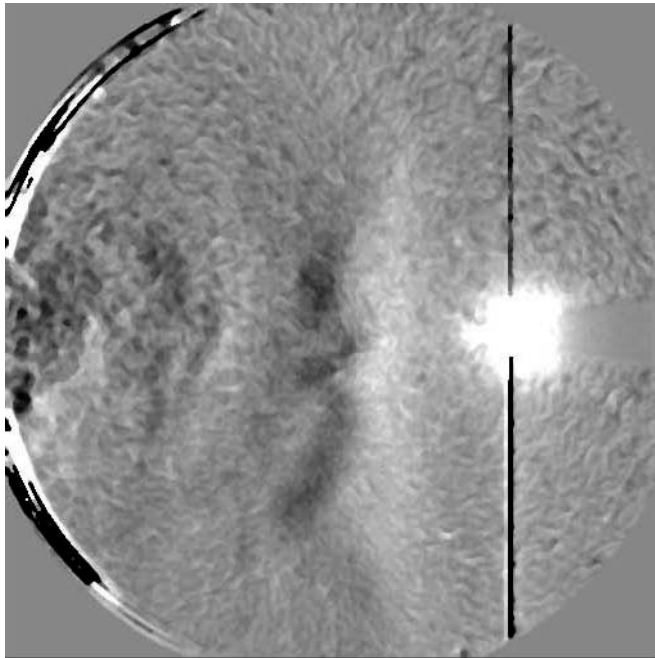


A cartoon illustrating the interaction of a shock with pre-existing turbulence.

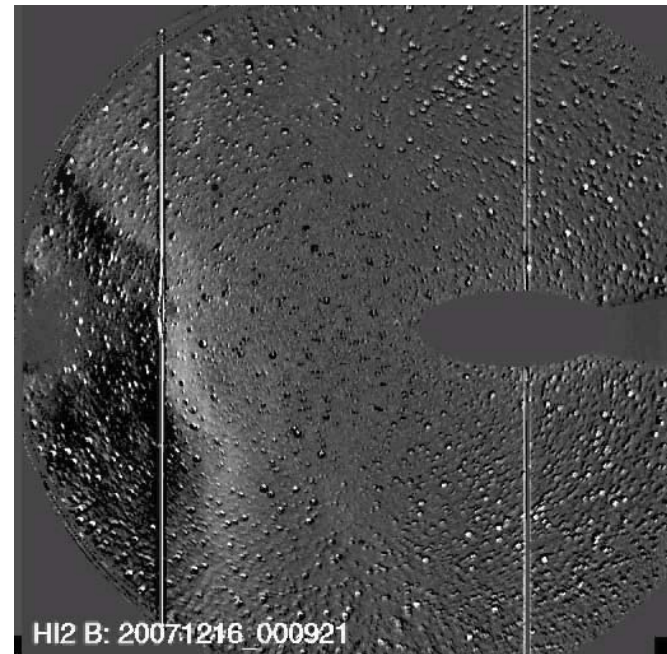


“rippled” interplanetary disturbances (STEREO/HI2 difference images)

May, 27 2008



Dec 16 2007

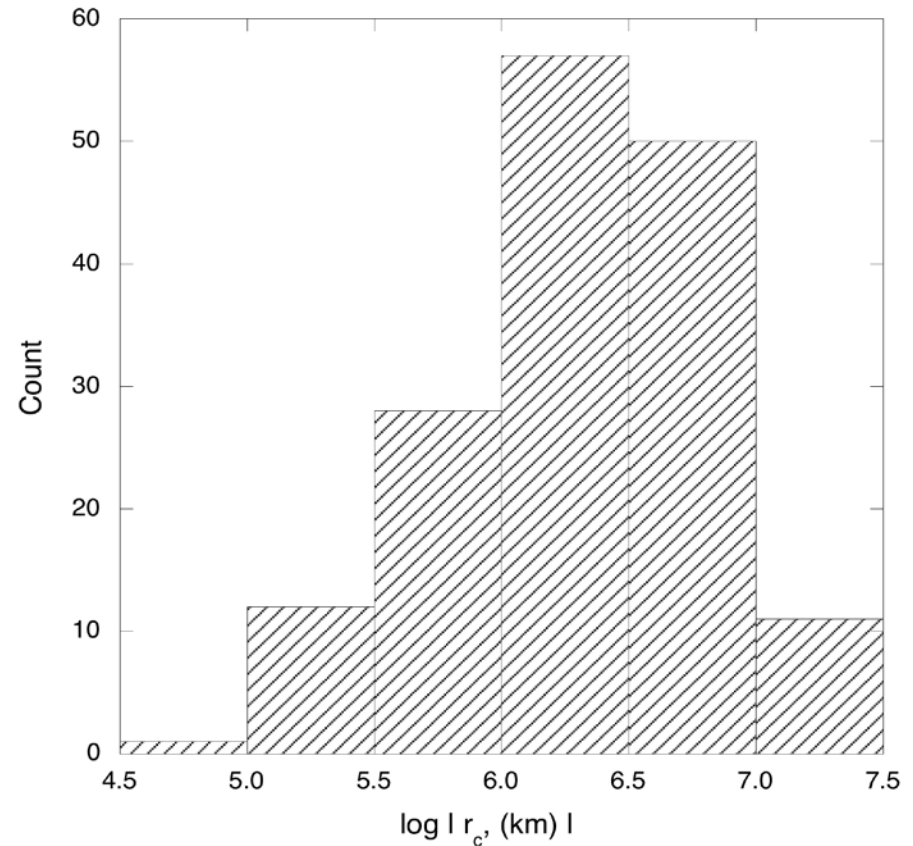
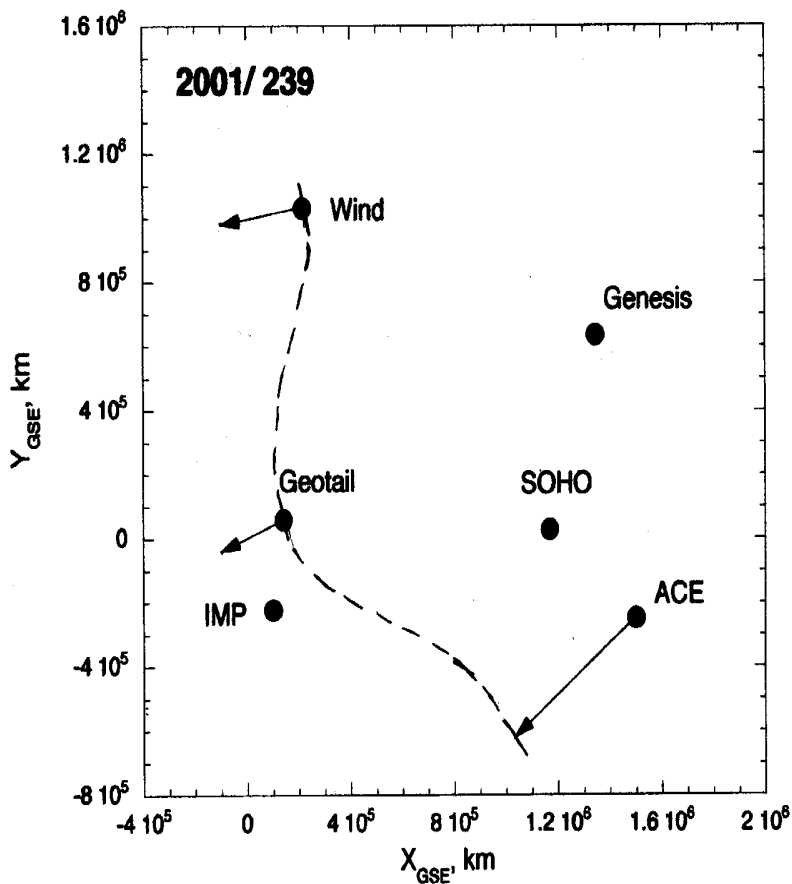


We at Arizona have suggested that many of the difficulties can be understood in terms of pre-existing, large-scale turbulence interacting with a shock.

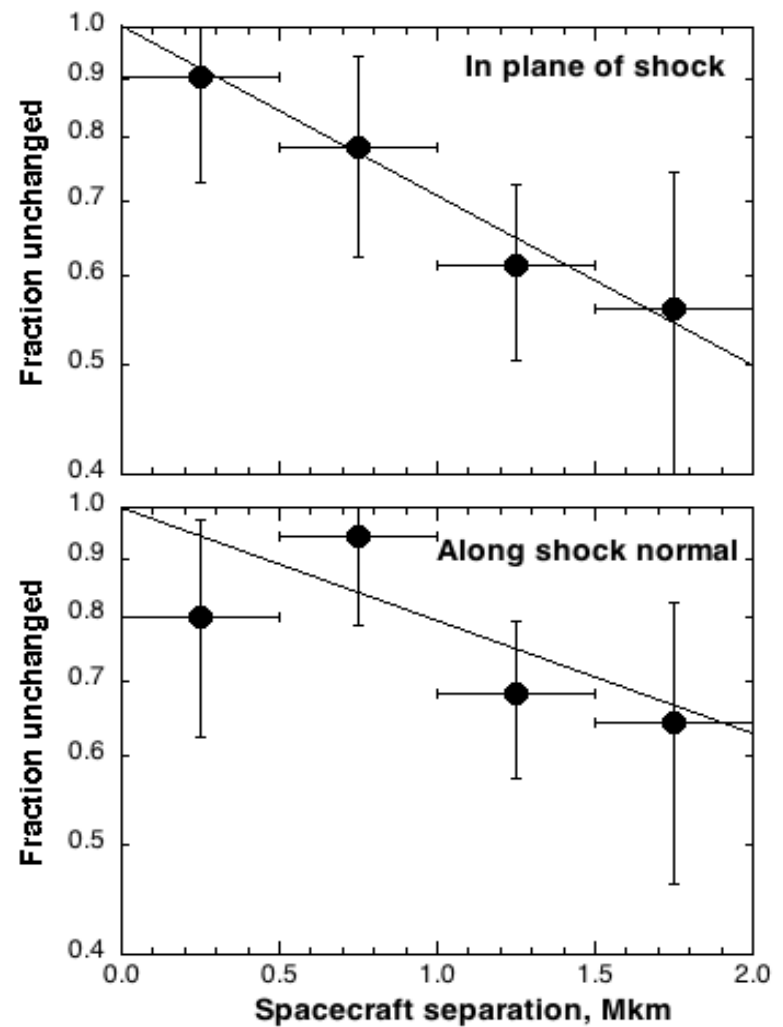
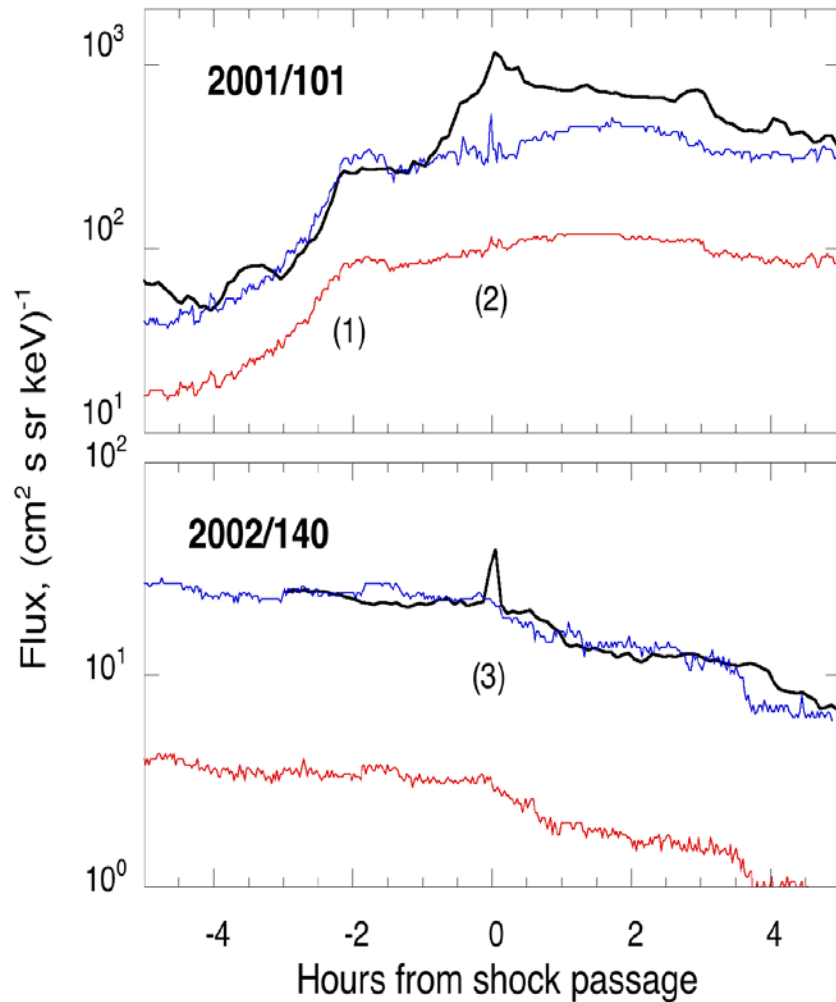
Multiple-Spacecraft Observations near Earth Allow Determination of Shock Shape and Normals (Giacalone and Neugebauer, 2005, 2007)

Example: Wind/Geotail saw this shock nearly simultaneously

Distribution of shock radii of curvature for many shocks



Example: Energetic particles also differ at different locations on the same shock.



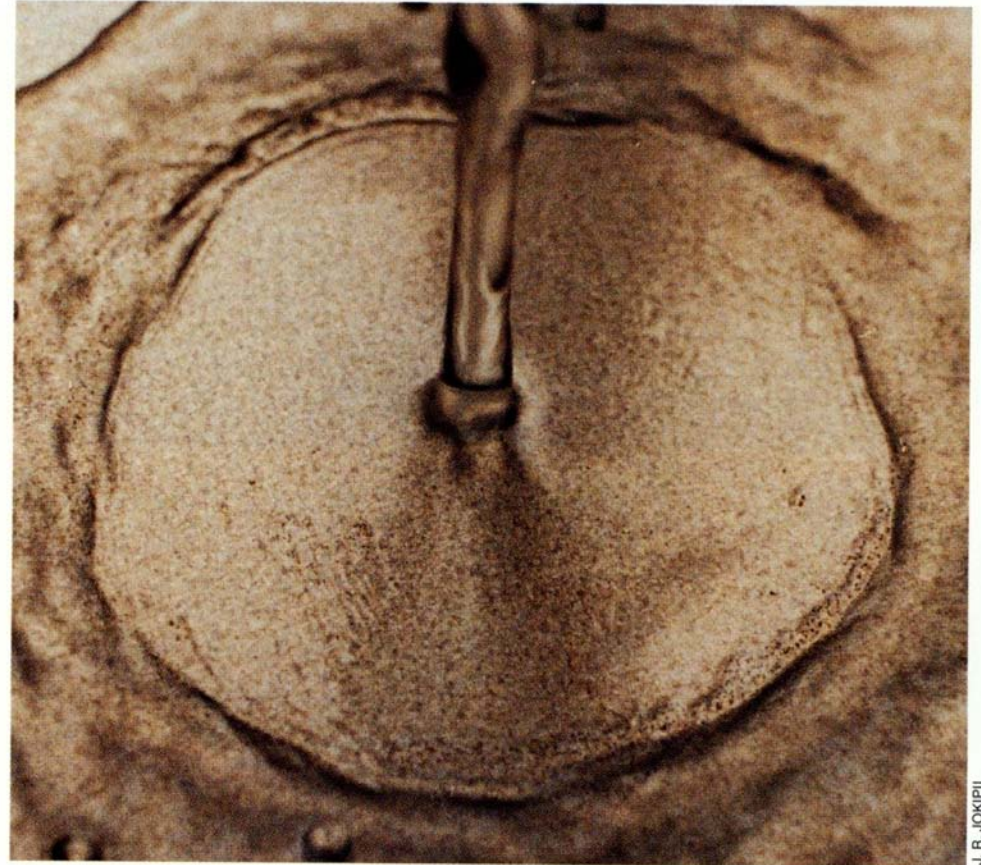
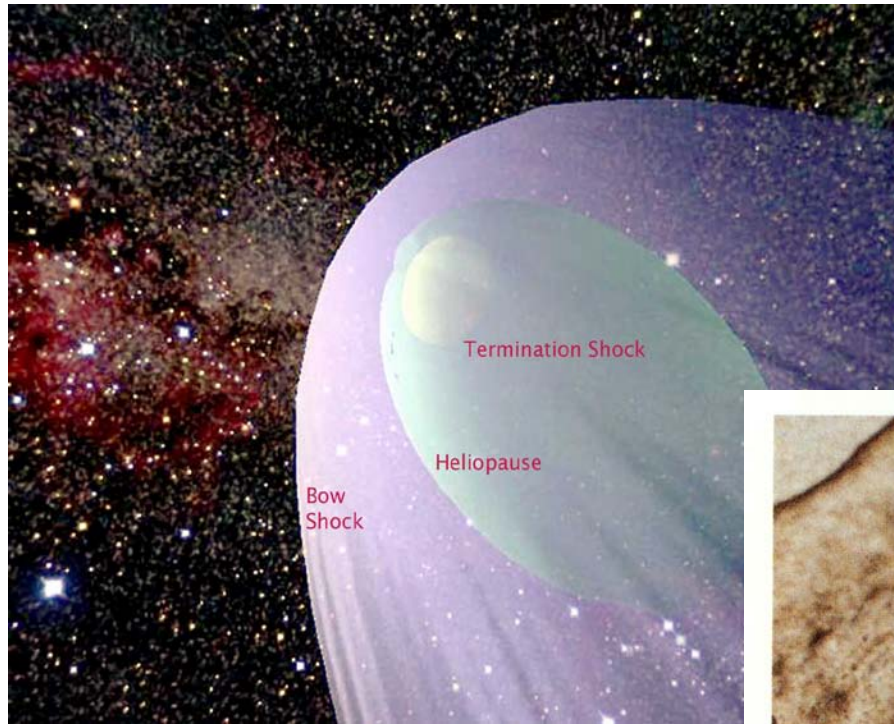
The coherence scale of the energetic-particle variations is about 1-2 million km.

This is the coherence scale of interplanetary turbulence.

Conclusions from these multi-spacecraft observations:

- Shock ripple radius of curvature = 2–3 Mkm.
- Persistence of EP features for $L \sim 3$ Mkm
- These are comparable to the correlation length of interplanetary magnetic field $\sim L_c \sim 2$ Mkm.
- We suggest that these are caused by pre-existing interplanetary turbulence.

The heliospheric termination shock shows similar behavior.

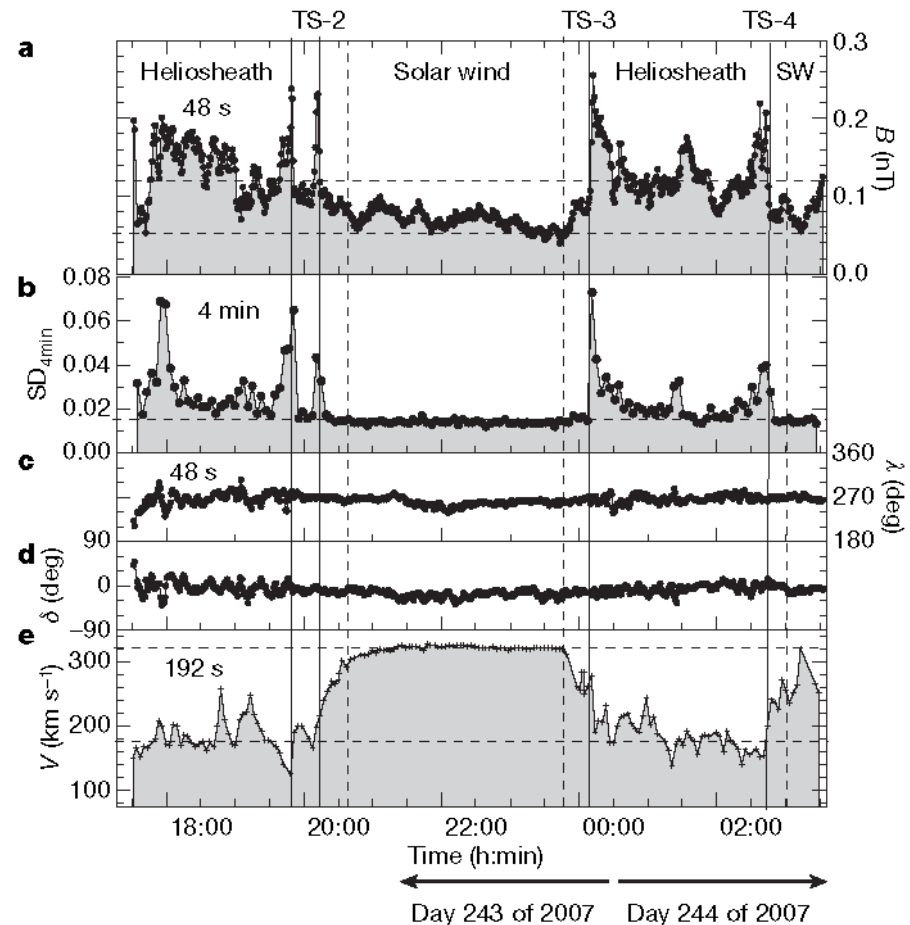


The kitchen sink analogue exhibits a turbulent termination shock, which Voyager 2 observed.

The Voyager 2 Termination Shock Crossing Provided Strong Evidence for such Turbulence

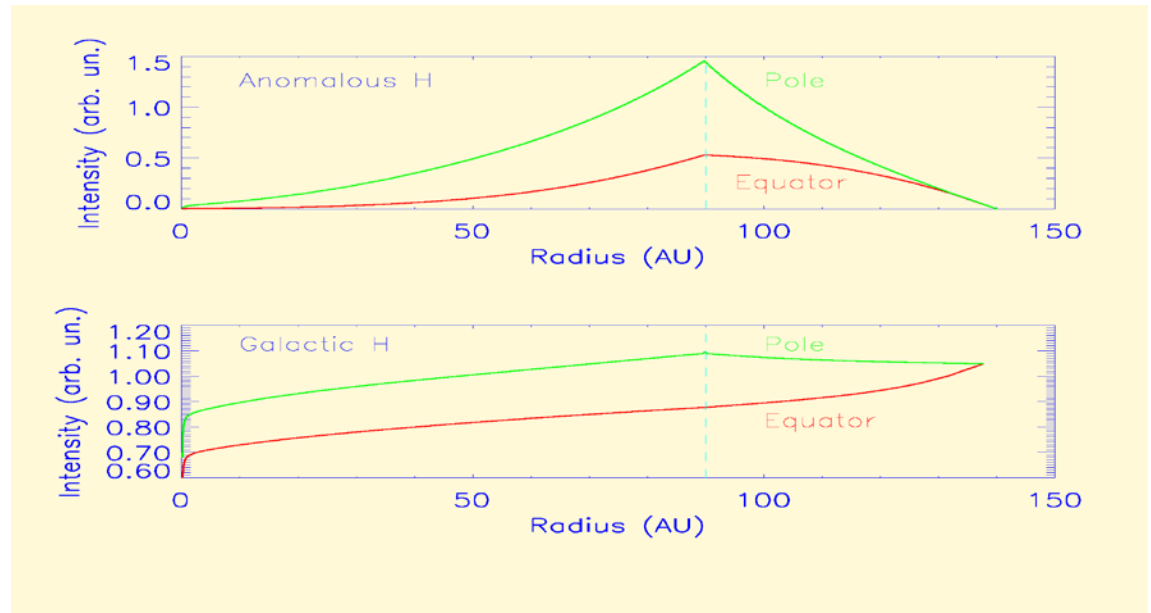
- The functioning plasma detector helped to provide richer data set than from V1.
- Also, the crossing was at a much slower shock speed.

The multiple shock crossings in a few days argued for a turbulent shock, moving back and forth irregularly.

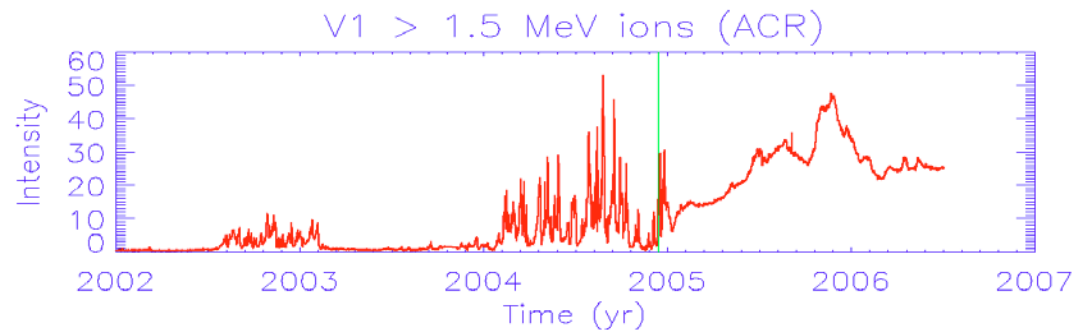


Anomalous cosmic rays are probably accelerated in this region.

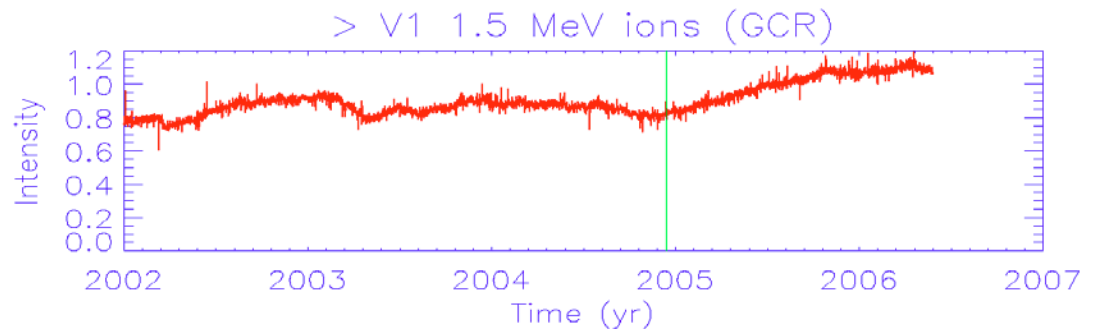
The radial dependence obtained from solving Parkers equation for a termination shock.



What was actually observed at the termination shock.



We attribute this discrepancy to turbulence hitting the shock..



Conclusions

- Collisionless shock waves are observed in the heliosphere from the Sun to the termination shock of the solar wind.
- They produce many different populations of energetic particles.
- Many of these, including the important termination shock, are nearly perpendicular shocks.
- Recent analyses suggest that many of the anomalies seen are the result of the shocks interacting with pre-existing, upstream turbulence.